Effect of Concentration on the Photo-Orientation and Relaxation Dynamics of Self-Assembled Monolayers of Mixtures of an Azobenzene-Based Triethoxysilane with Octyltriethoxysilane

ARTICLE *in* LANGMUIR · MARCH 2011

Impact Factor: 4.46 · DOI: 10.1021/la104457v · Source: PubMed

Langmuir

ARTICLE

pubs.acs.org/Langmuir

Effect of Concentration on the Photo-Orientation and Relaxation Dynamics of Self-Assembled Monolayers of Mixtures of an Azobenzene-Based Triethoxysilane with Octyltriethoxysilane

Guanjiu Fang, Nathan Koral, Chenhui Zhu, Youngwoo Yi, Matthew A. Glaser, Joseph E. Maclennan, and Noel A. Clark*

Department of Physics and the Liquid Crystal Materials Research Center, University of Colorado, Boulder, Colorado 80309, United States

Eva D. Korblova and David M. Walba

Department of Chemistry and Biochemistry and the Liquid Crystal Materials Research Center, University of Colorado, Boulder, Colorado 80309, United States

Supporting Information

ABSTRACT: Self-assembled monolayers (SAMs) were prepared from solutions with different proportions of a photoactive, azobenzene-based, silanized derivative of disperse red one (dDR1), and octyltriethoxysilane (OTE), a shorter, nonphotoactive molecule. The in-plane photoinduced orientational ordering of the resulting two component monolayers was monitored via precision measurement of in-plane birefringence using a dedicated high-extinction polarimeter. Measurements of contact angle, absorption, and birefringence show that introduction of OTE into the dDR1 deposition solution produces a continuous reduction of the surface density of dDR1 in the SAM, enabling the study of photowriting and relaxation dynamics in monolayers ranging from 100% dDR1 to samples where the dDR1 coverage is about 35%. The orientational dynamics depend strongly on the areal density of dDR1. As the fractional area of dDR1 is reduced, the rates of photowriting, photoerasing, and thermal relaxation increase, and the local orientational confinement of the molecules becomes more heterogeneous.

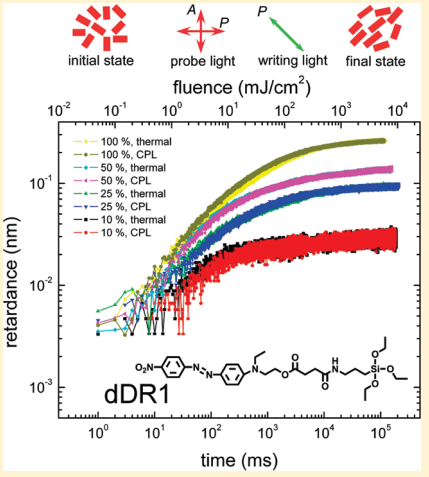

I. INTRODUCTION

Azobenzene and its derivatives undergo photoisomerization between trans and cis isomers in the presence of light. This transformation is reversible: the trans form can be converted into cis by illuminating with light, while the cis can be converted to trans either thermally or by light. Under irradiation with linearly polarized light (LPL) of suitable wavelength, the photoisomerization process is characterized by angle-dependent excitation that results in the photoselection of a preferred orientation of azobenzene dye molecules perpendicular to the polarization direction, so that the orientational distribution of azobenzene molecules becomes anisotropic.[1]

This photoinduced reorientation has been widely studied and developed in three-dimensional (3D) condensed phases, producing a variety of interesting optical and mechanical effects when the dye is incorporated into polymer[1−6] or liquid crystal media.[7] In addition to 3D systems, azobenzene-based monolayer thick films, both Langmuir−Blodgett[8−13] and self-assembled,[14−21] have been studied. Some azobenzene monolayers are liquid crystals (LCs) in 2D, exhibiting macroscopic orientational order that can be visualized by probing the textures of the in-plane birefringence, and photomanipulated using polarized light that applies an effective torque to the LC orientation field.[8,9] Other azobenzene monolayer systems are 2D isotropic phases in equilibrium, becoming anisotropic only when illuminated with polarized light,[11,16−21] Such photoinduced orientational order has been detected by UV/vis dichroism[16] and by monitoring the orientation of bulk liquid crystal in contact with the photo-oriented monolayer,[17−20] but detailed measurements of photo-induced monolayer anisotropy have not been possible.

Here we extend the direct observation of photoinduced in-plane orientational ordering of azobenzene-based SAMs, using a

Received: November 9, 2010
Revised: February 5, 2011
Published: March 14, 2011

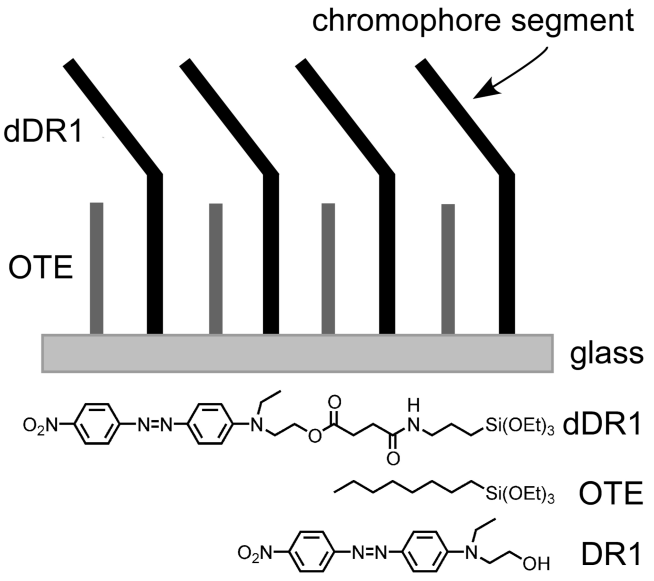

Figure 1. Chemical structures of dDR1 and OTE, and schematic picture of the formed mixed SAM made using a solution of dDR1 and OTE in toluene. The chromophores are localized at the air−SAM interface, and are tilted from the glass normal. The OTE molecules are used to control the surface density of the dDR1, providing additional free volume for the dDR1 molecules as the concentration of OTE is increased. The molecular structure of DR1 is also shown here for reference.

high contrast polarimeter,[22] capable of measuring monolayer birefringence as small as $\Delta n \sim 0.005$, that enables the quantitative characterization of partially ordered monolayers with partial surface coverage of the azobenene component, here as small as 35%. We measure, in monolayers that are isotropic in equilibrium, the saturation monolayer birefringence as a function of surface coverage, as well as the dynamics of orientational ordering when the monolayer is exposed to polarized actinic light, and its relaxation back to the 2D isotropic state when the light is removed.

The photo- and thermal isomerization rates of azobenzene dyes are known to depend strongly on environment in monolayers[10,11,14,15,23,24] and in polymer films (see the Supporting Information). If the fraction of the azobenzene component in a mixed monolayer is varied over a wide range, as in our case from 35% to 100% dDR1, the molecular environment can be expected to change substantially, and significant changes of the dynamic and steady state saturation ordering can be expected. For example, when azobenzene-based molecules are closely confined in dense monolayers on water[23,24] or in LB films,[11] photoisomerization is suppressed, with relatively few cis isomers present under illumination. Our experiments enable exploration of the effect of changing molecular confinement on the photo-orientation process in 2D.

Specifically, we describe the dependence on surface concentration of the photoreorientation dynamics of self-assembled monolayers (SAMs) made of mixtures of dDR1, a photoactive derivative of the azobenzene-based dye disperse red one, and octyltriethoxysilane (OTE), shown in Figure 1. As the concentration of OTE is increased relative to that of dDR1 in the deposition solution, the OTE increasingly dilutes the dDR1 in the SAMs formed. Because OTE is much shorter than dDR1, we expect that in a close-packed dDR1/OTE SAM where dDR1 is dilute, the photolabile portion of the dDR1 molecules will on the average protrude above the surrounding OTE molecules and will thus be relatively free to isomerize. As the dDR1 concentration is increased, the dDR1 molecular reorientation should become increasingly constrained.

II. EXPERIMENTAL SECTION

A. dDR1-SAM Preparation. The chemical structures of dDR1 ((*E*)-2-(ethyl(4-((4-nitrophenyl)diazenyl)phenyl)amino)ethyl 4-oxo-4-(3-(triethoxysilyl)propylamino)butanoate, a derivative of disperse red one), and octyltriethoxysilane (OTE) are shown in Figure 1. OTE is a commercial product from Gelest Inc., and was used as received.

The synthesis of dDR1 is as follows. Succinanhydride (1.28 g, 13 mmol) was suspended in 125 mL dry dichloromethane, and 3 mL (2.83 g, 13 mmol) of triethoxy(3-aminopropyl)silane was added. The suspension changed to clear solution and was stirred for 21 h at room temperature. Then 3 g (9.5 mmol) of disperse red 1 was added, followed by 3.21 g (16 mmol) of dicyclohexylcarbodiimide and a trace of 4-dimethylaminopyridine. The mixture was stirred for an additional 24 h at room temperature, the solid dicyclohexyl urea was filtered off, the residual solution was evaporated, and the crude product was purified by flash chromatograpy on silica gel (Merck 60, with activity 2−3 on the Brockmann−Schodder scale) using dichloromethane/5% ethanol mixture as eluent. Although the compound has some reactivity with silica, there is no catalyst as in the SAM preparation and we do not heat the column. Some material could be caught on the surface of the silica but most of it goes through. There was obtained 5.08 g (63%) of a dark red, solid compound with melting point 98−101 °C. NMR, mass spectrum, and elemental analyses are shown in the Supporting Information.

Before depositing SAMs on the glass slides, the substrates are first soaked for 1 h in piranha solution (1:1 concentrated H_2SO_4/30% H_2O_2). Then they are sonicated and rinsed several times in distilled or deionized water and blown dry with pure nitrogen gas. The cleaned substrates are extremely hydrophilic. The hydrolyzed surfaces readily form covalent bonds with the triethoxysilane groups in both dDR1 and OTE.

The preparation of the mixed dDR1-SAMs is carried out as follows: 0.574 mmol of the dDR1/OTE mixture is dissolved in 70 mL of toluene with 0.35 mL *n*-butylamine as a catalyst. The resulting solution is heated to about 45 °C while being sonicated to form a homeogeneous solution. A glass slide is put into the solution, which is further sonicated to prevent molecules from physically attaching on the glass. After 90 min, the substrate is taken out of solution and rinsed with toluene until the solvent no longer absorbs color during rinsing. Finally, the substrate is blown dry with pure nitrogen. We prepared SAMs using dDR1/OTE solutions containing 10, 25, 50, and 100 mol % dDR1. A schematic picture of the resulting mixed SAMs is shown in Figure 1.

B. Azo-SAM Cell. Azo-SAMs degrade if they are exposed simultaneously to air and light. We therefore constructed sealed cells filled with argon using two SAM-coated glass slides spaced about 5 μm apart.[21] Epoxy was used to seal the periphery, and the SAM monolayers were removed from the outer glass surfaces using piranha solution. Such cells, with SAMs solely on the inner glass surfaces in an inert argon atmosphere, were used to measure the reorientation dynamics of the monolayers.

C. Photobuffing Azo-SAMs. A high extinction polarimeter[22] was designed to measure the tiny birefringence changes induced in the SAMs by exposure to polarized light. This instrument uses a 0.7 mW helium−neon laser focused to a 40 μm diameter spot on the sample as the probe beam and has an extinction ratio of 2.4×10^{-10}. For photowriting the SAMs, two 514 nm pump beams, one of which is linearly polarized and the other circularly polarized, are incident on the cell with an angle of 10° with respect to the probe beam. The pump beams can be turned on or off

individually with 40 μs switching time by applying square waveforms to ferroelectric liquid crystal optical shutters. The pump beams are 1.67 mm in diameter, which is much wider than the probe beam, so that the probed region is essentially uniformly illuminated.

For an anisotropic organic monolayer between air and a substrate of index n_g, illuminated with visible light, the retardance is very small and the transmission T is well approximated by[22]

$$T \cong \left\{ \frac{\pi \Delta n d}{\lambda} \left[\frac{4 n_m}{(n_g + 1)^2} \right] \right\}^2 \sin^2 2\theta \qquad (1)$$

where a principal optic axis is along the mean in-plane molecular orientation of the monolayer n, θ is the angle between n and the polarization of the probe light, d is the film thickness, and $n_m = (n_\parallel + n_\perp)/2$ is the mean refractive index of the sample in the film plane. For a monolayer with optical anisotropy typical of a liquid crystal ($n_m = 1.6$, $n_g = 1.5$, and $\Delta n = 0.13$) we have $4n_m/(n_g + 1)^2 \sim 1$. With $\theta = 45°$ and assuming small Δnd, we can invert eq 1 to find the retardance $\Delta nd \approx (\lambda\sqrt{T})/\pi$.

III. RESULTS AND DISCUSSION

A. Monolayer Characteristics. Water contact angle measurements show that the SAMs become increasingly hydrophobic with decreasing dDR1 concentration c, where c is the mol % of dDR1 in the dDR1/OTE solution, as shown in Figure 2a. A pure OTE-SAM has a hydrophobic surface with a contact angle of $\beta = 89.5°$, while a pure dDR1-SAM is hydrophilic with a contact angle of $\beta = 68.6°$. The contact angle decreases by ~14° when c increases from 0 to 25%, with a further reduction of ~7° as c increases from 25 to 100%. This nonlinear dependence suggests that the hydrophilicity of the SAMs is dominated by the chromophores on the dDR1 molecules when c is greater than 25%. Cassie's law[25] predicts that the fractional area occupied by the dDR1 chromophore is given by

$$f = \frac{\cos\beta - \cos\beta_1}{\cos\beta_2 - \cos\beta_1} \qquad (2)$$

where f is the fractional area occupied by dDR1, β_1 and β_2 are the contact angles of pure OTE and dDR1 SAMs, respectively, and β is the contact angle on the two-component, heterogeneous surface. For solutions with c = 10, 25, and 50%, the calculated fractional areas of dDR1 chromophore in the mixed SAMs are 35, 69, and 79%, respectively, as shown in Figure 2a, from which we conclude that the SAM surface is more than 70% covered by the dDR1 chromophores and that deposition of dDR1 becomes less efficient as c increases above about 25%. The fractional area reflects the actual proportion of the glass covered with dDR1, rather than the concentration of dDR1 in the dDR1/OTE solution. The absorbance of randomly oriented dDR1-SAMs at 466 nm (see the Supporting Information for the visible absorption spectrum vs concentration) is found to be linearly proportional to the fractional area computed using Cassie's law as shown in Figure 2b, confirmation that the wetting angle measurements can be reliably used to obtain the relative number of dDR1 molecules in the SAM. AFM scans of the dDR1/OTE SAMs (see the Supporting Information) show that the SAMs exhibit a surface texture of domains of scale ~100 nm, with a root-mean-square roughness of ~2.7 nm at low c, becoming smoother as c increases. While we can control the overall fractional area of the surface covered by dDR1 (Figure 2a), the spatial distribution and correlation of the dDR1 and OTE domains is determined by

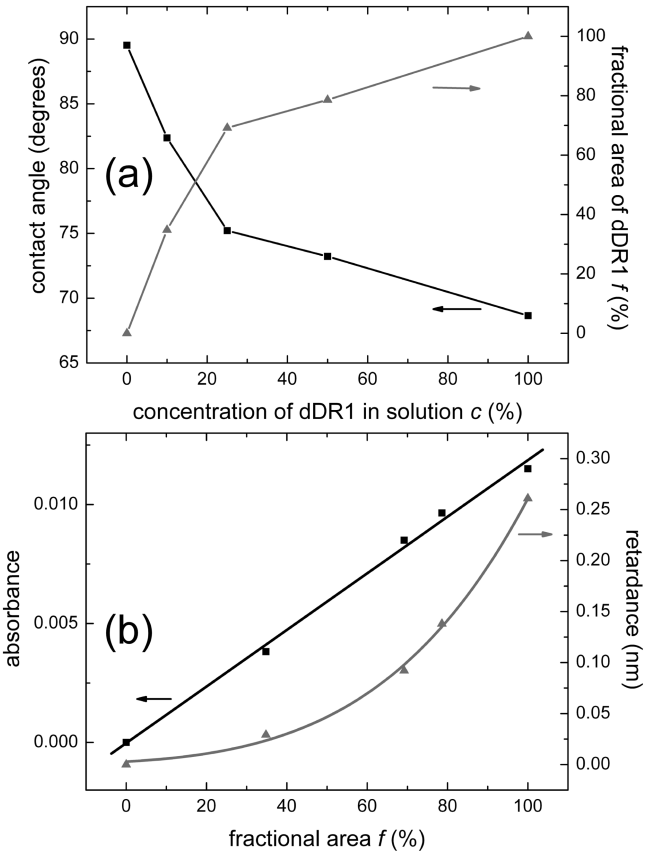

Figure 2. (a) Characteristics of dDR1-SAMs. Water contact angles (solid squares) and fractional area of dDR1 (f, solid triangles) on SAMs prepared with different concentrations of dDR1 in mixed dDR1/OTE solutions. f is calculated from water contact angles using Cassie's law. (b) Peak absorbance of the isotropic randomly oriented state and saturated retardance of the anisotropic written state versus f (writing fluence $F = 5$ J/cm^2, Figure 3a). The linear dependence of the isotropic state absorbance and the superlinear dependence of the saturated order on f suggests order enhancement by a cooperative orientation effect as the surface coverage of dDR1 increases.

the deposition and self-assembly processes and the intermolecular interactions. The domain size observed in the dDR1/OTE SAMs at c = 10% is very similar to that observed in deposition of SAMs of hydrocarbon silanes.[26]

B. Orientational Dynamics. *1. Photowriting.* The linearly polarized 514 nm pump beam is used to induce orientational anisotropy in SAMs containing dDR1 with initially random azimuthal orientation of the chromophores. During this writing process, the dDR1 molecules gradually become ordered along the direction normal to the incident light polarization, as sketched in Figure 3, and the birefringence of the monolayer increases from zero to some saturated value. Three principal processes control the induced anisotropy: angular hole burning (AHB), angular redistribution, and rotational Brownian diffusion of the molecules.[27−29] AHB results from the absorptive anisotropy of dye molecules, with their absorbance being strongest when the polarization of the exciting light is along the long axis, that is, along the transition dipole orientation of the chromophores. The molecules are selectively pumped according to their orientation, producing an anisotropic distribution of trans isomers and inducing birefringence in the monolayer. The cis

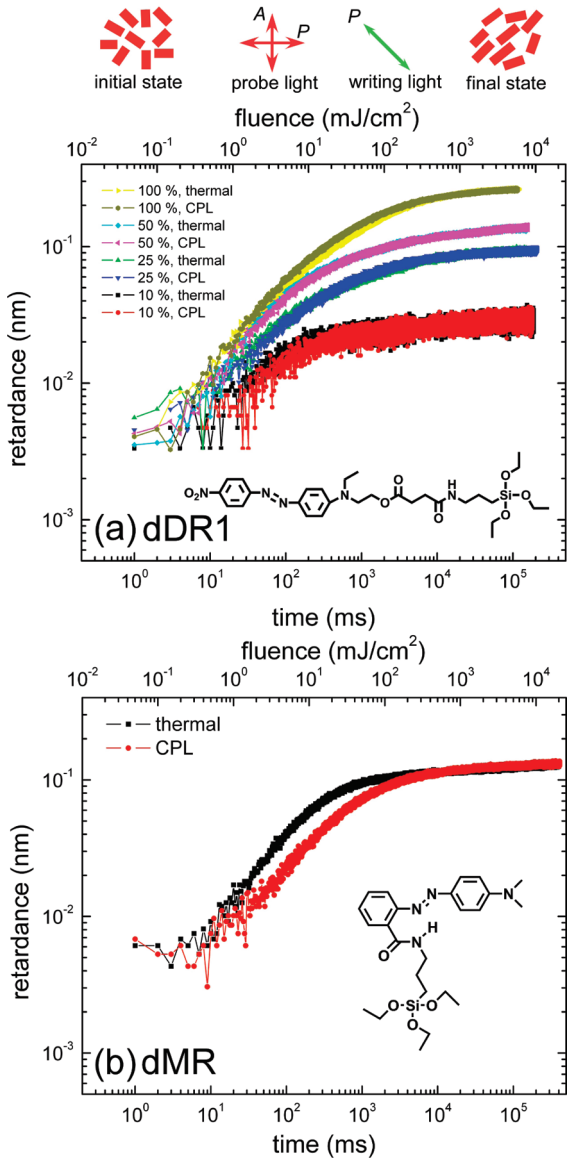

Figure 3. (a) Photowriting with linearly polarized light incident on dDR1-SAMs prepared with different concentrations of dDR1 in dDR1/OTE solution. The SAMs are initially azimuthally isotropic, a state created either by exposure to circularly polarized light (illumination with 50 mW/cm^2 CPL for 5 s) or by thermal relaxation. The linearly polarized writing light intensity is 50 mW/cm^2. The final director orientation of the SAM is at 45° to the crossed polarizer/analyzer of the probe beam. The pump and probe beam wavelengths are 514 and 632.8 nm respectively. (b) Photowriting dMR-SAMs with linearly polarized incident light, starting with isotropic states created either by exposure to circularly polarized light or by thermal relaxation as with dDR1. The writing conditions are the same as those in (a).

isomers generated are converted back into the trans form, either thermally or optically, with the resulting trans molecules appearing with an isotropic distribution of the orientation. This angular redistribution process provides trans isomers for the AHB process and amplifies the anisotropy created by AHB. After several trans−cis−trans cycles, there is an accumulation of trans isomers oriented perpendicular to the polarization of the exciting light. The axis of average trans orientation is defined as the director **n**. Rotational Brownian diffusion, on the other hand,

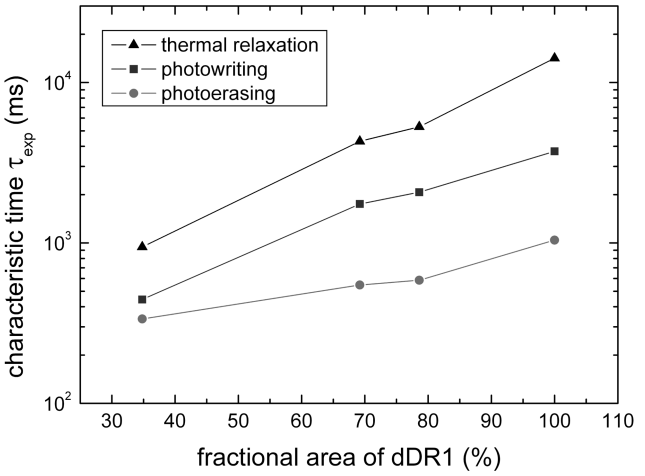

Figure 4. Characteristic times for SAM reorientation as a function of dDR1 fractional area. The plots show rise times for photowriting from the initial minimum retardance to ∼70% of the maximum value (squares), and decay times for thermal relaxation (triangles) and photoerasing (circles) from an initial maximum retardance (after 5 s exposure to LPL) to ∼30% of this value as a function of fractional area. The rise times are extracted from the writing curves shown in Figure 3a, and the decay times from the relaxation data in Figure 5.

tends to randomize the orientational distribution, repopulating orientationally depleted populations by thermal diffusion.

When SAMs containing dDR1 are illuminated with LPL, birefringence develops in the initially random surface and the transmission between crossed polarizers oriented at 45° to the incident polarization increases from zero to some saturated value. The increase in retardance Δnd, derived from the transmission data using eq 1, is shown for a typical set of experiments in Figure 3a. The birefringence induced by photoorientation is $\Delta n(t) = \Delta n_{max} S$, where Δn_{max} is the birefringence when all the molecules are completely ordered and S is the orientational order parameter. We have no independent measurements of Δn_{max} and S, but comparison can be made with the bulk azobenzene-based nematic liquid crystal DR1, which has $\Delta n_{max} \sim 0.4$.[7] Assuming an order parameter of about 0.6, this would give a saturated birefringence of 0.24, which is what we obtain. Figure 2b shows that the saturated retardance increases monotonically with f, confirming the increase of f with solution concentration c, but exhibits a superlinear dependence, in contrast with the linear variation versus f of the absorbance of the isotropic state. This suggests that there exists a cooperative orientation effect between molecules enabling larger saturated order parameter in the anisotropic written state as f increases. If, in Figure 3a, the retardance curves of c = 10% and 100% are scaled to the same saturation value (by shifting them up or down on the log plot), then it can be seen that the lower concentration curve in fact reaches its saturation value more quickly. We define the characteristic time τ_{exp} as the time for retardance to increase from the minimum to 70% of its maximum value, as shown in Figure 4. Photowriting of SAMs with higher dDR1 surface coverage proceeds more slowly than that for SAMs with lower surface coverage, as shown in Figure 4, evidence either that the orientational viscosity is increasing or that the isomerization is suppressed in the presence of dDR1 neighbors.

The rate at which orientational order appears during writing in these experiments is found to be essentially identical for both the

dx.doi.org/10.1021/la104457v |*Langmuir* 2011, 27, 3336–3342

thermally and optically induced random initial orientations for all dDR1 concentrations. This is in contrast to the behavior of a derivative of methyl red based SAMs (dMR-SAMs),[21] shown in Figure 3b, where the optically erased SAM responds more slowly to LPL. This difference may be due to the fact that in dDR1 the donor−acceptor groups have a low-lying $\pi-\pi^*$ state, giving a faster relaxation from cis to trans state than the methyl red molecule in the dMR-SAMs, so that only a small fraction of cis isomers is present in the dDR1-SAMs in the presence of circularly polarized light (CPL), slightly different from the thermally randomized state. In methyl red based monolayers, on the other hand, the fraction of cis in CPL-induced isotropic monolayers is larger, about 55% immediately after erasing.

2. Thermal and Photo-Driven Relaxation. SAMs that have been oriented with LPL can be randomized thermally or by exposing them to CPL. After exposure for some time to LPL, the dye molecules in the oriented SAM comprise both trans and cis isomers, with the ratio of trans to cis isomers in the steady state depending on the quantum yields of the isomerization reactions, the absorption coefficients of the two isomers at the irradiation wavelength, and the rate of thermal relaxation.[30] This steady state can be seen in Figure 3a and b, where the final saturated birefringence reaches the same value independent of how the initial state was prepared. The birefringence contribution from the cis isomers can be ignored because of their low optical anisotropy.[31]

Such an aligned azo-SAM spontaneously relaxes to a randomly oriented state through thermal fluctuations, with the induced birefringence decaying as the azimuthal distribution of trans isomers becomes isotropic, as shown in Figure 5a. The relaxation experiments are limited to room temperature, since, if the temperature is substantially changed from where the cells were assembled (room temperature), strain appears in the glass plates, leading to stray birefringence that swamps the optical signal of the monolayer. The typical time τ_{exp} for decay of the birefringence to 30% of its starting value is in the range $1s < \tau_{exp} < 14$ s, as shown in Figure 4. These times are many orders of magnitude longer than one would expect on the basis of single-molecule orientational diffusion in hydrocarbon milieu. This implies that the relaxation must be an activated process, with the molecules cooperatively trapped for long times in orientational wells separated from other orientations by energy barriers.

Aligned azo-SAMs can also be randomized by exposure to CPL. The resulting birefringence decrease during the erasing process, shown in Figure 5b, measures how quickly the orientationally ordered trans isomers are converted into cis. The angular redistribution of the cis isomers does not affect the birefringence since the trans isomers converted from the cis state appear with random azimuths and the exciting light is circularly polarized. Figure 5c compares the decay of birefringence for thermal and CPL erasure following LPL writing with a fluence $F = 250$ mJ/cm^2. The erasing dynamics depends on the surface composition, with τ_{exp} being the time taken to reduce the birefringence to ~30% of the initial value increasing with the fractional area of dDR1, as shown in Figure 4, which compares the thermal and photoerasing τ_{exp} values. Both show that erasure of the order proceeds more slowly with increasing surface coverage, with τ_{exp} for photoerasing ranging from three times smaller than that for thermal relaxation at 35% dDR1 fractional area to 14 times smaller at 100% fractional area. Thermal diffusion is thus less efficient than photoerasing at eliminating orientational order, especially at high dDR1 coverage, because it relies only on the azimuthal redistribution of trans isomers by orientational diffusion of the chromophores out of their ordered state, while in photoerasing azimuthal randomization is accelerated by photoinduced trans to cis photoisomerization. Figure S3 in the Supporting Information compares the decay for CPL erasure of starting LPL-written states generated by irradiation with

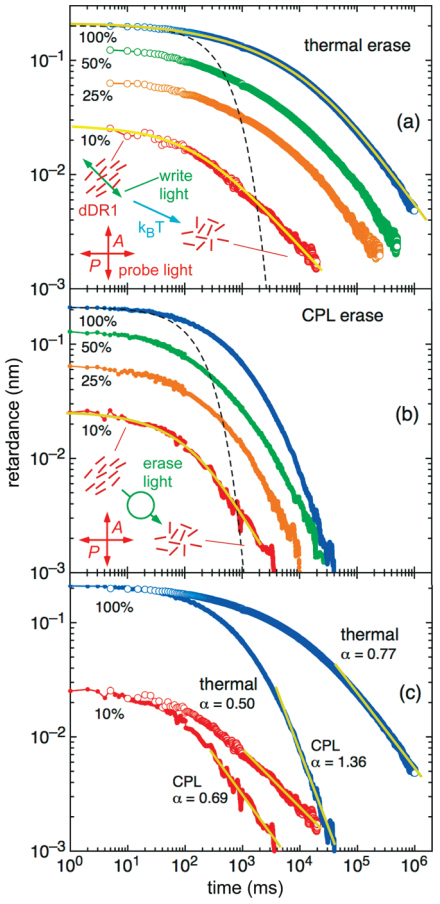

Figure 5. Relaxation of SAMs prepared with different concentrations of dDR1 in dDR1/OTE solution and oriented with LPL. The initial director orientation is at 45° with respect to the polarization of the probe beam. The initial fluence $F = 250$ mJ/cm^2 (the photoerasing dynamics for $F = 1250$ mJ/cm^2 is shown in Figure S3 in the Supporting Information.). The light intensity of photoerasing is 50 mW/cm^2. The pump and probe beam wavelengths are 514 and 632.8 nm, respectively. The curves as recorded relax to constant background intensity equivalent to $\Delta nd \sim 0.0001$ nm. This background has been subtracted from each curve. (a) Thermal relaxation of retardance for solution dDR1 concentration $c = 10$, 25, 50, and 100%. The dashed black curve is an exponential decay of Δnd, showing that the relaxations are qualitatively slower and glasslike. The yellow curves are fits to the Mittag−Leffler decay function, with the values of α indicated in (c). The decrease of α with decreasing dDR1 coverage indicated a broader distribution of relaxation times with decreasing dDR1 coverage. (b) CPL photoerasing is significantly faster than thermal but exhibits the same power-law symptotic behavior as thermal relaxation. (c) Comparison of thermal and photorelaxation at the low and high limits of dDR1 concentration in solution, showing the asymptotic slopes and values from the MLF fits. The overall decrease in α (increase in heterogeneity) with decreasing c is evident. For both values of c the decay exponent α is large for CPL erasure, an indication that once photon-assisted relaxation starts taking place the weakly trapped molecules readily move, causing the overall distribution of waiting times for diffusion to become narrower.

dx.doi.org/10.1021/la104457v |*Langmuir* 2011, 27, 3336–3342

$F = 250$ mJ/cm^2 with that of $F = 1250$ mJ/cm^2, showing that the rate at which the LPL-written surface is randomized by CPL decreases with increasing fluence. Harder initial writing by LPL thus generates stronger trapping in the written state.

The thermal- or CPL-induced loss of birefringence is a manifestation of an orientational diffusion process in which an anisotropic distribution of trans isomers, $f(\varphi,0)$, where φ is the in-plane orientation of the molecular long axis, set by the initial writing condition, relaxes to being isotropic in the plane, that is, $f(\varphi,t) = 1/2\pi$. Models developed for the Brownian diffusion of macroscopic objects subject to fluctuating thermal forces, for example, the Langevin equation,[32] enable calculation of the relaxation of $f(\varphi,t)$ and its moments $A_j(t)$, the coefficients in the harmonic expansion of $f(\varphi,t) = \Sigma_j A_j(t)\cos(j\varphi)$ in terms of the orthogonal functions $\cos(j\varphi)$.[33] In such a model, the decay of each coefficient is exponential and at long time only the $A_2(t)\cos(2\varphi)$ term remains,with its exponential decay rate being the smallest. The corresponding relaxation of $\Delta n(t)$ at long time is also exponential since $\Delta n(t) \propto \langle\cos(2\varphi)\rangle = A_2(t)$, where the average is over the distribution $f(\varphi,t)$. Figure 5a and b includes a fit of an exponential relaxation (dashed black lines) to typical $\Delta n(t)$ time series, showing the distinctly nonexponential nature of the birefringence decay in the dDR1 monolayer. By contrast, the solid yellow curves and lines overlaying the data, which characterize the asymptotic decay of Δn as an inverse power law in time, $\Delta n(t) \sim 1/t^{\alpha}$, describe the long-time behavior of both the thermal and CPL-driven relaxation well, and illustrate why such decay is considered "slow" relative to exponential decay.

The phenomenology of such nonexponential relaxation in condensed phases has been explored in the context of the mechanical and dielectric behavior of glassy materials,[34] and more generally in diffusive processes as a manifestation of the breakdown of the assumptions that lead to the classical models of Brownian motion.[35] The latter are generally based on calculation of the displacement and velocity of objects free to move but subject to a white-noise fluctuating force, which, with use of the central limit theorem, leads to Gaussian displacement statistics, Fick's law, the diffusion equation, and exponential relaxation.[32] Such a picture is not generally applicable to single or few molecule groups in materials where, for example, the molecules are maintained in a distribution of heterogeneous local structural situations for long periods of time, a typical situation encountered in glasses leading to nonexponential relaxation. In such cases, the diffusion process itself can be fundamentally altered. One useful approach to describe glassy diffusion is to consider Brownian motion as a series of random steps with a distribution of waiting times $w(\tau)$ between steps (the continuous time random walk)[36] and therefore an average waiting time $\tau_{ave} = \langle\tau\rangle$ over $w(\tau)$. If long waiting times occur with sufficient frequency, that is, if $w(\tau)$ falls sufficiently slowly with increasing τ, then τ_{ave} will be infinite, and the usual assumptions leading to the diffusion equation fail.[35] Specifically, if the waiting time distribution is taken to be the inverse power law $w(\tau) \sim 1/\tau^{1+\alpha}$, with $0 < \alpha < 1$, then the rotational diffusion equation $[\partial/\partial t]f(\varphi,t) = K[\partial^2/\partial\varphi^2]f(\varphi,t)$ will be replaced by the "fractional diffusion equation" $[\partial/\partial t]f(\varphi,t) = K\,[{}_oD_t^{1-\alpha}]\,[\partial^2/\partial\varphi^2]f(\varphi,t)$, where $[{}_oD_t^{1-\alpha}]$ is the Riemann−Liouville operator for fractional order time differentiation.[35] Separation of variables yields relaxation behavior with time dependence for each harmonic in φ given by Mittag−Leffler functions, $E_\alpha(-[t/t_{oj}]^\alpha)$, where the t_{oj} are separation constants.[37] Again, the lowest order harmonic $\cos(2\varphi)$ has the largest t_{oj} so that the long-time behavior of the birefringence is given by $\Delta n(t) \propto \langle\cos(2\varphi)\rangle \propto E_\alpha(-[t/t_o]t^\alpha)$, where t_o is a characteristic time.[37] The Mittag−Leffler function (MLF) decays for small t as a stretched exponential $E_\alpha(-[t/t_o]^\alpha) \sim \exp\{-[t/t_o]^\alpha/\Gamma(1+\alpha)\}$ and at large t as an inverse power law, $E_\alpha(-[t/t_o]^\alpha) \sim 1/\{[t/t_o]^\alpha\Gamma(1-\alpha)\}$, where $\Gamma(x)$ is the gamma function. The birefringence is of the form $\Delta n(t) = CE_\alpha(-[t/t_o]^\alpha)$, so that C and t_o are scaling constants, respectively, displacing the calculated $\Delta n(t)$ vertically or horizontally on a log−log plot such as those in Figure 5. The single parameter α is the only one affecting the shape of $\Delta n(t)$, setting its asymptotic slope. Figure 5a and b show typical MLF fits to the dDR1 thermal and CPL relaxation curves, and Figure 5c gives the fitted values of the asymptotic slope α versus coverage for thermal and CPL erasing. As can be seen, α is the smallest for thermal relaxation at the lowest dDR1 coverage and increases with increasing coverage and increasing erasing intensity. Thus, at low coverage, the distribution of waiting times is much broader than that at higher coverage. Since the high coverage case has a larger τ_{exp} (Figure 4), it must be the local structures with shorter waiting time that are preferentially eliminated as coverage is increased. CPL increases the slopes somewhat relative to those of thermal erasing, indicating that the effectiveness of the photon assist apparently increases with waiting time. Comparison of the CPL erasing dynamics for writing fluences of 250 and 1250 mJ/cm^2 in Figure S3 in the Supporting Information shows that α decreases with increasing fluence. Thus, as the writing becomes harder, the lifetime of the oriented molecular clusters achieved is extended to larger values, leading to a broader distribution of waiting times and thus smaller values of α.

Figure 4 shows an increase of roughly an order of magnitude in the characteristic writing and erasing τ_{exp} for dDR1 as its fractional coverage on the two-dimensional surface is increased from 35% to 100% of the area. In 3D, the corresponding variation in characteristic reorientation times of a molecule such as DR1 would be much larger, as it would be isotropic in solution when dilute, with submicrosecond reorientation times at the low end of this concentration range, and nematic at the high end,[38] with arbitrarily slow, collective reorientation modes. With this in mind, we might have expected to observe a much stronger dependence of characteristic times in the mixed SAMs than that seen in Figure 4. We attribute the less dramatic dependence in the SAMs to (i) the segregation into domains of primarily OTE and primarily dDR1 indicated by the AFM experiments, which would have the effect of reducing the difference in molecular environment of the chromophores at low and high coverage; and (ii) the effects of reduced dimensionality, which limit the extent of achievable orientational ordering.

IV. CONCLUSIONS

The availability of a polarimeter capable of making precision measurements of the birefringence of monolayers of small molecules with liquid-crystal-like in-plane ordering has enabled the study of the dependence of photoinduced alignment of azobenzene-based SAMs as a function of surface coverage. Quantitative birefringence measurements, at chromophore coverage as low as 35% in fractional area, probe the behavior of photoactivity in SAMs over an unprecedented range of surface coverage. Observation of photowriting dynamics, and the decay of birefringence induced thermally or by illumination with circularly polarized light, shows that increasing the surface density of photoactive dDR1 molecules in mixed dDR1/OTE

SAMs slows all of these processes. The saturated photoinduced birefringence increases more rapidly than chromophore coverage, indicating an increasing tendency for collective ordering at high coverage. Full coverage dDR1 monolayers show a narrower distribution of relaxation times for orientational diffusion than those with partial coverage, which are more heterogeneous in this regard.

■ ASSOCIATED CONTENT

Supporting Information. Discussion of azobenzene photoisomerization, chemical characterization of the synthesized dDR1 molecule, AFM images and absorption spectra of SAMs, and further information on SAM photoerasing dynamics. This material is available free of charge via the Internet at http://pubs.acs.org.

■ ACKNOWLEDGMENT

This work was supported by NSF MRSEC Grant DMR-0820579 and NSF Grant CHE-0508520.

■ REFERENCES

(1) Todorov, T.; Nikolova, L.; Tomova, N. *Appl. Opt.* **1984**, *23*, 4309.
(2) Brown, D.; Natansohn, A.; Rochon, P. *Macromolecules* **1995**, *28*, 6116.
(3) Rochon, P.; Batalla, E.; Natansohn, A. *Appl. Phys. Lett.* **1995**, *66*, 136.
(4) Yu, Y.; Nakano, M.; Ikeda, T. *Nature* **2003**, *425*, 145.
(5) Ikeda, T.; Sasaki, T.; Ichimura, K. *Nature* **1993**, *361*, 428.
(6) Gibbons, W. M.; Shannon, P. J.; Sun, S.-T.; Swetlin, B. J. *Nature* **1991**, *351*, 49.
(7) Aronzon, D.; Levy, E. P.; Collings, P. J.; Chanishvili, A.; Chilaya, G.; Petriashvili, G. *Liq. Cryst.* **2007**, *34*, 707.
(8) Ignés-Mullol, J.; Claret, J.; Albalat, R.; Crusats, J.; Reigada, R.; Romero, M. T. M.; Sagués, F. *Langmuir* **2005**, *21*, 2948.
(9) Burriel, P.; Ignés-Mullol, J.; Reigada, R.; Sagués, F. *Langmuir* **2006**, *22*, 187.
(10) Nakagawa, M.; Watase, R.; Ichimura, K. *Mol. Cryst. Liq. Cryst.* **2000**, *344*, 113.
(11) Schönhoff, M.; Mertesdorf, M.; Lösche, M. *J. Phys. Chem.* **1996**, *100*, 7558.
(12) Haro, M.; Gascón, I.; Aroca, R.; López, M. C.; Royo, F. M. *J. Colloid Interface Sci.* **2008**, *319*, 277.
(13) Seki, T.; Sakuragi, M.; Kawanishi, Y.; Suzuki, Y.; Tamaki, T.; Fukuda, R. I.; Ichimura, K. *Langmuir* **1993**, *9*, 211.
(14) Tamada, K.; Akiyama, H.; Wei, T. X. *Langmuir* **2002**, *18*, 5239.
(15) Sekkat, Z.; Wood, J.; Geerts, Y.; Knoll, W. *Langmuir* **1996**, *12*, 2976.
(16) Sekkat, Z.; Wood, J.; Geerts, Y.; Knoll, W. *Langmuir* **1995**, *11*, 2856.
(17) Ichimura, K.; Suzuki, Y.; Seki, T.; Hosoki, A.; Aoki, K. *Langmuir* **1988**, *4*, 1214.
(18) Aoki, A.; Seki, T.; Suzuki, Y.; Tamaki, T.; Hosoki, A.; Ichimura, K. *Langmuir* **1992**, *8*, 1007.
(19) Ichimura, K.; Hayashi, Y.; Akiyama, H.; Ikeda, T.; Ishizuki, N. *Appl. Phys. Lett.* **1993**, *63*, 449.
(20) Yi, Y. W.; Farrow, M. J.; Korblova, E.; Walba, D. M.; Furtak, T. E. *Langmuir* **2009**, *25*, 997.
(21) Fang, G.; Shi, Y.; Maclennan, J. E.; Clark, N. A.; Farrow, M. J.; Walba, D. M. *Langmuir* **2010**, *26*, 17482.
(22) Fang, G.; Maclennan, J. E.; Clark, N. A. *Langmuir* **2010**, *26*, 11686.
(23) Iwamoto, M.; Majima, Y.; Naruse, H.; Iriyama, K. *J. Appl. Phys.* **1992**, *72*, 1631.
(24) Majima, Y.; Kanai, Y.; Iwamoto, M. *J. Appl. Phys.* **1992**, *72*, 1637.
(25) (a) Cassie, A. B. D. *Discuss. Faraday Soc.* **1948**, *3*, 11. (b) Liu, Y.; Wolf, L. K.; Messmer, M. C. *Langmuir* **2001**, *17*, 4329.
(26) Schwartz, D. K.; Steinberg, S.; Israelachvili, J.; Zasadzinski, J. A. N. *Phys. Rev. Lett.* **1992**, *69*, 3354.
(27) Pedersen, T. G.; Johansen, P. M. *Phys. Rev. Lett.* **1997**, *79*, 2470.
(28) Pedersen, T. G.; Johansen, P. M.; Holme, N. C. R.; Ramanujam, P. S.; Hvilsted, S. *J. Opt. Soc. Am. B* **1998**, *15*, 1120.
(29) Delaire, J. A.; Nakatani, K. *Chem. Rev.* **2000**, *100*, 1817.
(30) Rau, H. *Photochemistry and Photophysics*; Rabek, J. F., Ed.; CRC Press: Boca Raton, FL, 1990; Vol. 11, Chapter 4.
(31) Pedersen, T. G.; Ramanujam, P. S.; Johansen, P. M.; Hvilsted, S. *J. Opt. Soc. Am. B* **1998**, *15*, 2721.
(32) Reif, F. *Fundamentals of Statistical and Thermal Physics*; McGraw Hill: New York, 1965; Chapter 15.5.
(33) Berne, B. J.; Pecora, R. *Dynamic Light Scattering*; Wiley: New York, 1976.
(34) Jäckle, J. *Rep. Prog. Phys.* **1986**, *49*, 171.
(35) Metzler, R.; Klafter, J. *Phys. Rep.* **2000**, *339*, 1.
(36) Montroll, E. W.; Scher, H. *J. Stat. Phys.* **1973**, *9*, 101.
(37) Kalmykov, Y. P. *Phys. Rev. E* **2004**, *70*, 051106.
(38) Stinson, T. W.; Litster, J. D. *Phys. Rev. Lett.* **1970**, *25*, 503.